Developmental synaptic regulator, TWEAK/Fn14 signaling, is a determinant of synaptic function in models of stroke and neurodegeneration

Dávid Nagy[a,b] ⓘ, Katelin A. Ennis[c] ⓘ, Ru Wei[d] ⓘ, Susan C. Su[c], Christopher A. Hinckley[e], Rong-Fang Gu[d], Benbo Gao[d], Ramiro H. Massol[e] ⓘ, Chris Ehrenfels[e] ⓘ, Luke Jandreski[a], Ankur M. Thomas[c], Ashley Nelson[c], Stefka Gyoneva[c], Mihály Hajós[a,f], and Linda C. Burkly[c,1]

[a]Clinical Sciences, Biogen, Cambridge, MA 02142; [b]Biogen Postdoctoral Scientist Program, Cellular Physiology, Biogen, Cambridge, MA 02142; [c]Genetic and Neurodevelopmental Disease Research, Biogen, Cambridge, MA 02142; [d]Chemical Biology and Proteomics, Biogen, Cambridge, MA 02142; [e]Translational Cellular Sciences, Biogen, Cambridge, MA 02142; and [f]Comparative Medicine, School of Medicine, Yale University, New Haven, CT 06520

Identifying molecular mediators of neural circuit development and/or function that contribute to circuit dysfunction when aberrantly reengaged in neurological disorders is of high importance. The role of the TWEAK/Fn14 pathway, which was recently reported to be a microglial/neuronal axis mediating synaptic refinement in experience-dependent visual development, has not been explored in synaptic function within the mature central nervous system. By combining electrophysiological and phosphoproteomic approaches, we show that TWEAK acutely dampens basal synaptic transmission and plasticity through neuronal Fn14 and impacts the phosphorylation state of pre- and postsynaptic proteins in adult mouse hippocampal slices. Importantly, this is relevant in two models featuring synaptic deficits. Blocking TWEAK/Fn14 signaling augments synaptic function in hippocampal slices from amyloid-beta–overexpressing mice. After stroke, genetic or pharmacological inhibition of TWEAK/ Fn14 signaling augments basal synaptic transmission and normalizes plasticity. Our data support a glial/neuronal axis that critically modifies synaptic physiology and pathophysiology in different contexts in the mature brain and may be a therapeutic target for improving neurophysiological outcomes.

synaptic transmission | synaptic plasticity | Fn14 | stroke | TWEAK

Neural circuit patterning, refinement, and plasticity are enabled by the dynamic strengthening, weakening, and pruning of chemical synapses in response to circuit activity. However, synapse loss and reduced plasticity are early hallmarks of chronic neurological disorders such as autism, schizophrenia and Alzheimer's disease (AD) (1–3). It is therefore hypothesized that the underlying molecular mechanisms of pruning, although normally balanced in health, are dysregulated in disease. Particularly interesting is the notion that the mechanisms responsible for the reduction in functional synapses in disease reflect the aberrant reactivation of pathways important for synapse elimination in development. For example, in an AD model, synapse elimination was shown to be mediated by the complement pathway in the hippocampus (HC), reflecting aberrant reactivation of complement-dependent synapse elimination that occurs in the dorsal lateral geniculate nucleus (dLGN) of the thalamus during visual development (4). In such a paradigm, the reactivation of developmental mechanisms enables pathways that can act universally across different ages, circuits, and brain regions. Thus, the mechanisms underlying normal circuit development and their potential reactivation as key contributors to neurological diseases are areas of deep interest.

In addition to chronic neurological disorders, circuitry changes also occur in acute ischemic stroke, the second leading cause of death worldwide and a cause of debilitating long-term disability. Interruptions in blood flow that deprive neurons of oxygen and nutrients result in significant cell death, followed by deficits in

neurophysiological activity that are associated with poor motor recovery (5). Remarkably, the adult brain can undergo some degree of spontaneous poststroke recovery, apparently by engaging neuroplasticity mechanisms including remapping, synaptogenesis, and synaptic strengthening (5, 6). Despite these adaptations, over half of ischemic stroke patients fail to recover completely and continue to experience persistent long-term disability (7). The underlying signaling pathways that regulate synaptic physiology after stroke are an active topic of investigation.

TNF-like weak inducer of apoptosis (TWEAK) protein, originally discovered as a cytokine produced by macrophages (8), signals through its injury-inducible transmembrane receptor, FGF-inducible molecule-14 (Fn14) (9). Consequently, the function of TWEAK/Fn14 signaling was elucidated as a driver of tissue remodeling in contexts of injury and disease in a variety of organ systems (10). Recently, findings have suggested a role for the TWEAK/Fn14 pathway in the central nervous system (CNS). Namely, several compelling observations indicate that TWEAK

Significance

It is of great importance to elucidate mechanisms underlying the loss or dysfunction of synapses in neurological diseases. The concept that reduced functional synapses in disease reflect aberrant reactivation of pathways mediating synapse elimination in development has yielded candidate mechanisms. Here, we elucidate a role of the cytokine TWEAK and its receptor Fn14, previously shown to be critical in visual development, in synaptic function in the adult brain. We show that limiting this signaling pathway augments synaptic function in models of Alzheimer's disease and ischemic stroke. Our results support a general role of TWEAK/Fn14 signaling as a regulator of synaptic function across different ages and brain regions, highlighting it as a therapeutic target in diseases featuring synaptic dysfunction.

signaling through Fn14 might be a key molecular modulator of synaptic function in contexts of neurological challenge. TWEAK and Fn14 are up-regulated in the CNS in AD (11, 12, 13 and *SI Appendix*, Fig. S6A) and after ischemic stroke in humans and mice (14–16). Importantly, TWEAK/Fn14 signaling was also recently shown to be a pathway necessary for synapse maturation during experience-dependent visual development. Light-induced up-regulation of Fn14 in thalamocortical excitatory neurons and corresponding up-regulation of TWEAK in microglia mediate the elimination of weak synapses and strengthening of remaining synapses in the dLGN (17, 18). Indeed, the communication between neurons and supporting microglia has emerged as a key mechanism regulating neuronal circuitry, with microglia deploying their ramified processes to continuously survey and refine synapses in response to neural activity. Interestingly, TWEAK expression has also been shown to be microglia-enriched in the mouse cortex (19), suggesting that it may play a role in multiple brain regions. Thus, like the complement pathway, the TWEAK/Fn14 pathway could be an important regulator of synapse biology in visual development which is re-engaged and acts generally in different ages and brain regions to contribute to pathology.

The involvement of TWEAK/Fn14 signaling in synapse physiology or pathophysiology outside of the developing visual system is unknown. We considered it to be a strong candidate modifier of synaptic function in adults given that Fn14 is up-regulated and required for synaptic refinement in experience-dependent visual development, and TWEAK and Fn14 are up-regulated in contexts of neurological injury/disease, suggesting that the TWEAK/Fn14 system is tuned to periods of substantial change in neuronal activity levels or environment (e.g., eye opening, ischemic stroke). We employed HC slices to test the hypothesis that the TWEAK/Fn14 pathway regulates synaptic function in adult mice and in different disease contexts and delineate its mechanism of action. Herein, we reveal that TWEAK, through neuronal Fn14, mediates acute dampening of basal synaptic transmission and synaptic plasticity in hippocampal slices from mature mice. Furthermore, we demonstrate that TWEAK/Fn14 signaling broadly impacts the phosphorylation state of critical synaptic proteins, suggesting a general role in synapse modulation. Finally, we show that pathway deficiency or pharmacological inhibition of TWEAK/Fn14 signaling augments synaptic transmission and plasticity in amyloid-beta (Aβ)–overexpressing mice and post ischemic stroke animals, two model systems featuring synaptic functional deficits. Thus, our results support that TWEAK/Fn14 constitutes a synaptic regulatory pathway with therapeutic potential for CNS disorders in the adult brain.

Results

TWEAK Acutely and Dose-Dependently Attenuates Basal Synaptic Neurotransmission and Plasticity in Hippocampus. In order to evaluate the effect of TWEAK on basal synaptic neurotransmission and synaptic plasticity, we recorded the amplitudes of dendritic field excitatory postsynaptic potentials (fEPSP) in the hippocampal CA1 region in response to Shaffer collateral stimulation (Fig. 1A), using HC slices from naive, young (6 to 8 wk old) C57BL/6 mice. After establishing a 10-min baseline period, Fc-TWEAK or control protein were washed onto the slices for 30 min. The Fc-TWEAK wash-in caused an acute and dose-dependent reduction in basal synaptic neurotransmission (Fig. 1B). The mid (0.5 µg/mL) and high (1 µg/mL) doses resulted in an acute decrease in fEPSP amplitudes, usually reaching a plateau phase of attenuation 20 min later. Quantification showed attenuation of 21 and 27%, respectively, compared to the baseline amplitudes (Fig. 1C). The control protein (1 µg/mL) and the lowest tested dose of Fc-TWEAK (0.1 µg/mL) had no significant effect. Importantly, both Fc-TWEAK and agly-Fc-TWEAK, a form of TWEAK with an inactive Fc region, comparably and

significantly decreased basal synaptic neurotransmission relative to the control protein-treated group (*SI Appendix*, Fig. S1 B and C), confirming that TWEAK is the active component of the fusion protein rather than the Fc domain.

We next investigated whether the attenuation of synaptic transmission by TWEAK activity is reversible by incorporating a wash-out period. Indeed, the normalized fEPSP amplitudes gradually increased and returned to the baseline levels within 20 min after wash-out of the protein was initiated (*SI Appendix*, Fig. S1F). These results indicate that the acute dampening of basal transmission by TWEAK is not due to cell death.

Attenuated synaptic transmission could be secondary to TWEAK-induced changes in cell health, metabolism, and/or ion homeostasis. Therefore, to identify signaling proteins and molecular mechanism(s) underlying the dampening effects of TWEAK, we examined whether TWEAK induced phospho-proteomic changes in our brain slice model. Using a tandem mass tag (TMT) labeling-coupled proteomics workflow on brain slice homogenates (*SI Appendix*, Fig. S2 A and B), we quantified 20,774 phosphopeptides mapping to 4,340 proteins. We found that the phosphorylation of 269 proteins (*SI Appendix*, Table S1) significantly changed after 30 min of Fc-TWEAK exposure (0.5 µg/mL). MetaCore enrichment analysis on these 269 TWEAK-changed phosphoproteins identified "synaptic contact" as the most significantly enriched process network (false discovery rate [FDR]: 1.1e-3), and "synapse part" as the most enriched gene ontology localization (FDR: 6.8e-30) (*SI Appendix*, Table S2, A and B). These results link the modulation of synaptic strength by Fc-TWEAK to the molecular machinery of synaptic transmission.

To examine the effects of TWEAK on hippocampal synaptic plasticity, we induced long-term potentiation (LTP) using theta-burst stimulation (TBS) after the 30-min Fc-TWEAK or control protein wash-in period. At all three tested doses (0.1, 0.5, and 1 µg/mL), pretreatment with Fc-TWEAK resulted in a significantly lower LTP induction compared to the control protein-treated (1 µg/mL) group (Fig. 1 D and E). Pretreatment with agly-Fc-TWEAK had an effect comparable to that observed with Fc-TWEAK (*SI Appendix*, Fig. S1 D and E).

To mechanistically separate the effects of Fc-TWEAK on basal neurotransmission and synaptic plasticity, we increased the amplitudes of the fEPSPs in TWEAK-exposed slices to the baseline levels, by elevating the extracellular calcium concentration. In these conditions, synaptic plasticity was significantly lower in the baseline-adjusted Fc-TWEAK-treated group as compared to the control protein-treated group (*SI Appendix*, Fig. S1I). This result suggests that TWEAK can modulate LTP magnitude independent of its dampening of basal synaptic transmission.

Taken together, these findings indicate that Fc-TWEAK wash-in acutely and dose-dependently dampens basal synaptic neurotransmission through reversible mechanisms, decreases the inducibility of LTP, and modulates synaptic phosphoprotein signaling. Because the 0.5-µg/mL Fc-TWEAK was the lowest dose that significantly decreased both the basal synaptic neurotransmission and synaptic plasticity, we used this dose in all subsequent experiments.

TWEAK Dampens Synaptic Function through Neuronal Fn14. To test our hypothesis that the TWEAK receptor Fn14 is required for the modulation of synaptic functions by Fc-TWEAK, we first employed constitutive Fn14 knockout (Fn14KO) mice as a tool to globally inhibit Fn14 signaling (20). After determining that Fn14 deficiency causes no gross anatomical, histological, or functional changes in the cortex or hippocampus in adult mice (*SI Appendix*, Fig. S3 A–G), we tested the effects of Fc-TWEAK on brain slices from Fn14KO animals. We observed that the significant dampening of fEPSP amplitudes and LTP in wild-type (WT) slices by Fc-TWEAK was no longer evident in Fn14KO
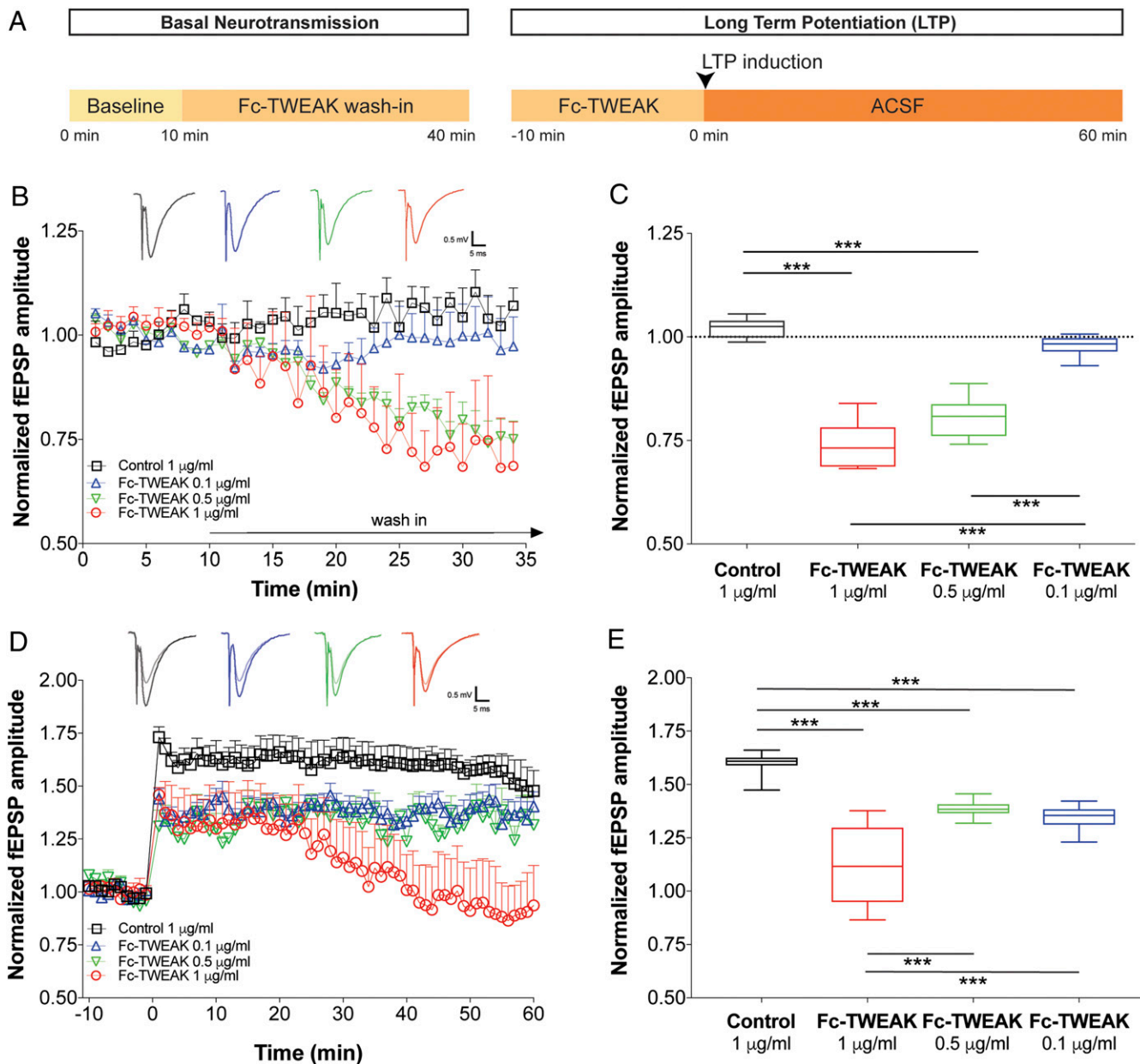
Fig. 1. TWEAK acutely and dose-dependently attenuates basal synaptic transmission and plasticity in the hippocampus. (*A*) Schematic time line of compound wash-in and electrophysiological recordings. HC slices were prepared from 6- to 8-wk-old male and female C57BL/6 WT mice. *n* = 5 to 6 slices/group. (*B*) Relative changes in basal neurotransmission following ex vivo wash-in of control protein or Fc-TWEAK. Group means plotted ± SEM. (*Insets*) Representative fEPSP traces from the various doses tested. (*C*) Quantification of the changes in basal neurotransmission after control protein or Fc-TWEAK wash-in. Box plots show the minimum to maximum values and means of the last 10 min of the wash-in period. Dotted line indicates the prewash-in baseline levels. One-way ANOVA, Tukey's multiple comparisons test. ***$P \le 0.001$. (*D*) Time line of LTP recordings following ex vivo wash-in of control protein or Fc-TWEAK. Group means plotted ± SEM. (*Insets*) Representative fEPSP traces from the various doses tested. Semitransparent traces represent signals from baseline, while solid traces show post-TBS signals. (*E*) Quantification of the LTP recordings following ex vivo wash-in of control protein or Fc-TWEAK. Box plots show the minimum to maximum values and means of the 10- to 50-min period after LTP induction. One-way ANOVA, Tukey's multiple comparisons test. ***$P \le 0.001$.

slices, indicating that Fn14 is required for the attenuation of basal synaptic neurotransmission (Fig. 2 *A–D*). Consistent with these observations, we found that 89.2% of TWEAK-induced synaptic phosphoproteomic changes were dependent on Fn14 (*SI Appendix*, Table S1). Overall, our results suggest that TWEAK impacts synaptic transmission via Fn14.

Next, we interrogated the cell-type specificity of Fn14 signaling using a viral strategy to isolate the role of neuronal Fn14 in mature brain circuits. We designed viral constructs of short-hairpin RNA (shRNA) targeting Fn14 or scrambled control sequence under

control of a neuron-specific promoter synapsin (PHP.eB-hSYN1-GFP-shTnfrsf12a and PHP.eB-hSYN1-GFP-shScrambled vectors, respectively) and injected them into postnatal day 0 (P0) neonatal pups to generate neuronal Fn14 knockdown (nFn14KD) and nScr mice, respectively (Fig. 2*E*). Using immunofluorescence, we found colocalization of 89% of GFP-expressing cells with the neuronal marker NeuN (Fig. 2*F*), but no visible colocalization with the astrocyte marker GFAP (*SI Appendix*, Fig. S4*A*). Furthermore, in situ hybridization showed that the Fn14 expression was significantly reduced in neuronal nuclei, but not in other nuclei, in nFn14KD
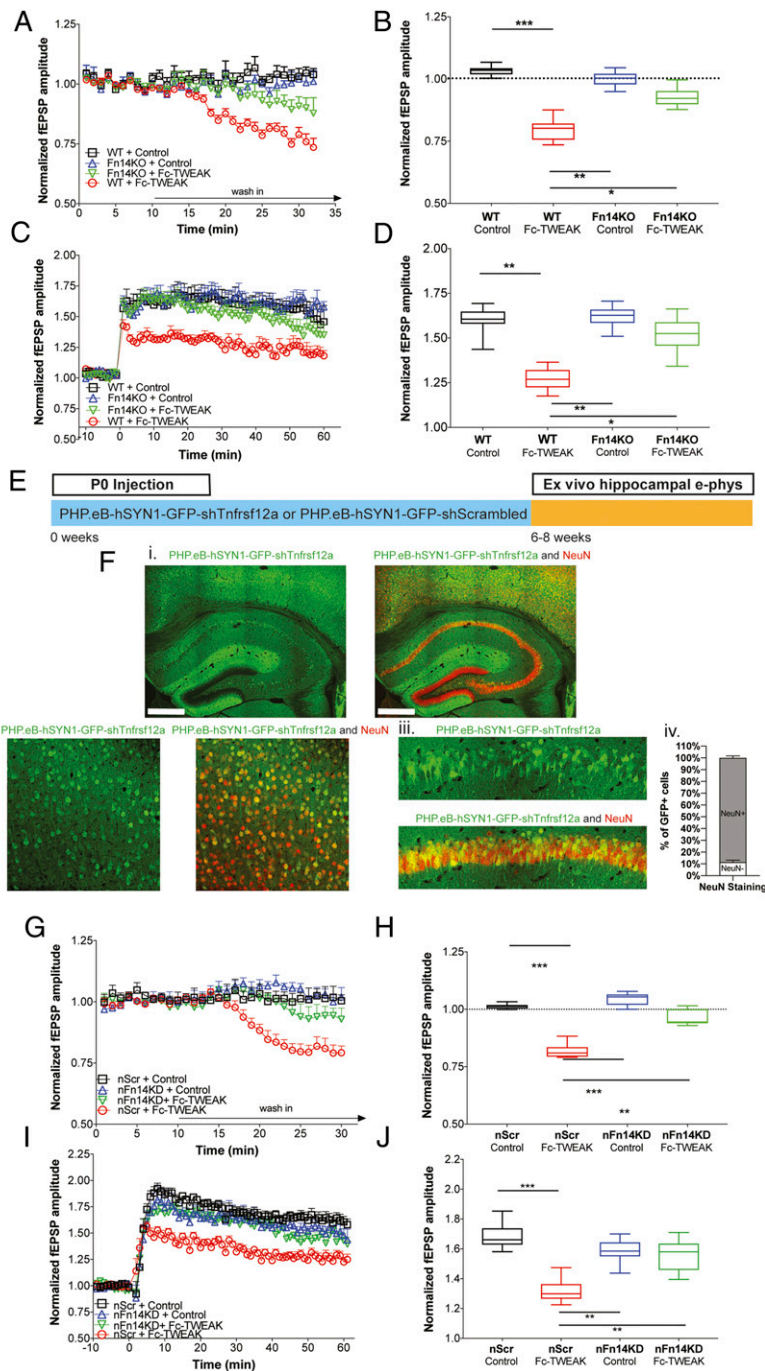
Nagy et al.
Developmental synaptic regulator, TWEAK/Fn14 signaling, is a determinant of synaptic function in models of stroke and neurodegeneration

PNAS | 3 of 11
https://doi.org/10.1073/pnas.2001679118

Fig. 2. Neuronal Fn14 is required for TWEAK attenuation of synaptic transmission and plasticity. (*A–D*) HC slices were prepared from 6- to 8-wk-old male and female WT or Fn14KO mice and treated with control protein (1 μg/mL) or Fc-TWEAK (0.5 μg/mL). *n* = 8 slices/group. (*A*) Relative changes in basal neurotransmission following wash-in. Group means plotted ± SEM. (*B*) Quantification of the changes in basal neurotransmission following wash-in. Box plots show the minimum to maximum values and means of the last 10 min of the wash-in period. Dotted line indicates the prewash-in baseline levels. One-way ANOVA, Tukey's multiple comparisons test. *$P \leq 0.05$, **$P \leq 0.01$, ***$P \leq 0.001$. (*C*) Time line of LTP recordings following wash-in. Group means plotted ± SEM. (*D*) Quantification of the LTP recordings following wash-in. Box plots show the minimum to maximum values and means of the 10- to 50-min period after LTP induction. One-way ANOVA, Tukey's multiple comparisons test. *$P \leq 0.05$, **$P \leq 0.01$. (*E*) Schematic of P0 injection of PHP.eB-hSYN1-GFP-shTnfrsf12a or PHP.eB-hSYN1-GFP-shScrambled vectors. HC slices were prepared from 6- to 8-wk-old animals. (*F*) Representative immunofluorescence images of GFP (green) expressed from PHP.eB-hSYN1-GFP-shTnfrsf12a viral vector and the neuronal marker NeuN (red). Images show low magnification of the hippocampus and cortex (i), and high magnification of the cortex (ii) and CA1 region of the hippocampus (iii). (Scale bar, 500 μm.) Plot shows proportion of GFP+ cells colocalized with the neuronal marker NeuN (iv). Means plotted ± SEM. *n* = 6 animals/group. (*G–J*) HC slices were prepared from 6- to 8-wk-old male and female nFn14KD or nScr mice and treated with control protein (1 μg/mL) or Fc-TWEAK (0.5 μg/mL). *n* = 8 slices/group. (*G*) Relative changes in basal neurotransmission following wash-in. Group means plotted ± SEM. (*H*) Quantification of the changes in basal neurotransmission after wash-in. Box plots show the minimum to maximum values and means of the last 10 min of the wash-in period. Dotted line indicates the prewash-in baseline levels. One-way ANOVA, Tukey's multiple comparisons test. **P value ≤ 0.01, ***$P \leq 0.001$. (*I*) Time line of LTP recordings following wash-in. Group means plotted ± SEM. (*J*) Quantification of the LTP recordings following wash-in. Box plots show the minimum to maximum values and means of the 10- to 50-min period after LTP induction. One-way ANOVA, Tukey's multiple comparisons test. **$P \leq 0.01$, ***$P \leq 0.001$.

Nagy et al.
Developmental synaptic regulator, TWEAK/Fn14 signaling, is a determinant of synaptic
function in models of stroke and neurodegeneration

mice (*SI Appendix*, Fig. S4*B*). Together, these results confirm the neuronal selectivity of the targeting vector.

Consistent with the data from the global Fn14KO mice, Fc-TWEAK treatment in nFn14KD mice failed to significantly decrease either basal synaptic transmission or LTP compared to Fc-TWEAK–treated nScr mice or control protein treatment groups (Fig. 2 *G–J*). Together, these observations suggest that Fc-TWEAK attenuates the basal synaptic neurotransmission and synaptic plasticity in a neuronal Fn14-specific manner in adult mice.

Thus far, we present evidence that TWEAK/Fn14 signaling dampens synaptic function through neuronal Fn14. This raised the possibility that these synaptic effects may be generated via NF-κB signaling (10), an established downstream effector of Fn14. Therefore, we implemented a computational approach to identify putative mediators between TWEAK/Fn14 and their synaptic targets identified by phosphoproteomic analysis. We built a protein interaction network based on TWEAK, Fn14, and the 12 TWEAK/Fn14-changed phosphoproteins in the most highly enriched network, i.e., synaptic contact, identified by MetaCore enrichment (*SI Appendix*, Table S2, C and D). This analysis identified a set of nine proteins, including Rac1 and Traf2, linking Fn14 to multiple TWEAK/Fn14-altered synaptic phosphoproteins (*SI Appendix*, Fig. S2*C*). In contrast, Fn14 signaling through NF-κB appeared to influence only a single synaptic protein. Taken together, these analyses suggest that TWEAK/Fn14 signaling impacts synaptic function primarily through non–NF-κB pathways.

TWEAK Attenuates Synaptic Transmission through Presynaptic Mechanisms. To further investigate the dampening effects of Fc-TWEAK on synaptic physiology, we next asked whether the activation of TWEAK/Fn14 signaling acts via pre- and/or postsynaptic mechanisms. To address this question, we used two independent approaches: measuring presynaptic neurotransmitter release probability in acute HC slices by calculating the paired-pulse ratio (PPR), as well as recording spontaneous single-unit activity in cultured mouse neurons after TWEAK wash-in. PPR, which is the ratio of the second fEPSP amplitude to that of the first, depends on the probability of vesicular release at the presynaptic site (21). We found that Fc-TWEAK treatment significantly increased the PPR of CA3 to CA1 fEPSPs at the shortest 25-ms interstimulus interval (ISI) compared to its own baseline or to the control treatment group, indicating decreased neurotransmitter release probability (Fig. 3 *A* and *B*). In addition, whole-cell recordings of miniature excitatory postsynaptic currents (mEPSCs) of dissociated primary mouse neurons revealed that a 30-min period of Fc-TWEAK exposure significantly reduced the frequency, but not the amplitudes, of spontaneous mEPSCs (Fig. 3 *C* and *D* and *SI Appendix*, Fig. S5), a change best described by a reduction in presynaptic release probability (22, 23). Taken together, the results from two independent electrophysiological approaches suggest that Fc-TWEAK treatment modulates synaptic transmission through a presynaptic mechanism(s).

Blocking TWEAK Augments Basal Synaptic Transmission and Plasticity in Aged WT and Tg2576 Hippocampal Slices. Having shown a role for TWEAK/Fn14 signaling in synaptic function, we next evaluated its potential involvement in disease models. The expression of Fn14 has been shown to be significantly increased in several brain regions of AD patients (*SI Appendix*, Fig. S6*A*). Thus, we employed aged Tg2576 mice, a commonly used AD model featuring synaptic deficits due to amyloid-beta overexpression (24, 25). We confirmed reduced basal transmission (*SI Appendix*, Fig. S6*B*) and reduced plasticity at the initial phase after LTP induction in aged Tg2576 mice as compared to WT mice. We therefore probed whether TWEAK/Fn14 signaling regulates synaptic function in hippocampal slices from aged Tg2576 and WT mice in a study design (Fig. 4*A*) similar to that used above.

Interestingly, Fc-TWEAK caused an acute and significant decrease in fEPSP amplitudes in brain slices from 9-mo-old WT (~22%, Fig. 4*B*) and Tg2576 (~18%, Fig. 4*C*) animals compared to their control protein-treated groups, with no difference between the genotypes (Fig. 4*D*). In addition, to address whether endogenous TWEAK can modulate synaptic transmission and plasticity in brain slices from aged Tg2576 and WT mice, we employed a monoclonal antibody (mAb) that binds TWEAK and blocks its interaction with Fn14. Blocking endogenous TWEAK/Fn14 signaling by anti-TWEAK mAb significantly increased fEPSP amplitudes (~15%) in both WT (Fig. 4*B*) and Tg2576 (Fig. 4*C*) slices compared to their control protein-treated groups, without genotype differences (Fig. 4*E*). This enhancement of synaptic activity by anti-TWEAK supports the relevance of endogenous TWEAK in the regulation of synaptic transmission.

Next, we investigated the potential effect of TWEAK/Fn14 on synaptic plasticity in aged 9-mo old Tg2576 and WT animals (Fig. 4 *F* and *G*). We found that slices from Tg2576 mice exhibit a significant deficit in synaptic potentiation, however, only at the initial stage after LTP induction (0 to 10 min post TBS) as compared to age-matched WT mice (Fig. 4*H*). Activation of Fn14 signaling by Fc-TWEAK significantly reduced LTP to a similar extent in both genotypes relative to their control protein-treated groups (Fig. 4*H*), while anti-TWEAK treatment significantly improved the deficit at the induction phase of LTP (Fig. 4*I*). These observations are not accounted for by genotype differences in Fc-TWEAK or anti-TWEAK wash-out (*SI Appendix*, Fig. S7).

Given the similar effect of TWEAK/Fn14 modulation in WT and Tg2576 mice, we examined Fn14 expression in the hippocampus of Tg2576 animals. Consistent with our synaptic recordings, we found that Fn14 expression was comparable in 9-mo-old Tg2576 and age-matched WT HC slices (*SI Appendix*, Fig. S6*C*). Although TWEAK/Fn14 synaptic regulatory effects are not enhanced in the Tg2576 hippocampus, these data suggest that endogenous TWEAK/Fn14 signaling retains its synaptic regulatory role in the context of aging and amyloid-beta overexpression and that inhibition of the pathway can rescue synaptic deficits induced by aging and/or disease.

Disruption of TWEAK/Fn14 Signaling Is Protective from Synaptic Transmission and Plasticity Deficits Emerging after Ischemic Stroke. Ischemic stroke is a disease state that features elevated levels of TWEAK and Fn14 in humans and mouse models (14–16). Given our findings revealing the TWEAK/Fn14 pathway as a modulator of synaptic function in the adult brain, we hypothesized that activation of TWEAK/Fn14 signaling after ischemic brain challenge may contribute to the delayed neurophysiological deficits that follow.

To test the role of the TWEAK/Fn14 pathway on stroke-induced synaptic deficits, we leveraged the distal middle cerebral artery occlusion + hypoxia (DH-MCAO) mouse model of ischemic stroke which manifests delayed impairment in hippocampal neuronal activity after infarction of the somatosensory cortex (26) detectable at 8 and 14 wk post stroke (*SI Appendix*, Fig. S8 *A–G*). The model also features increased TWEAK and Fn14 expression in this delayed time frame (Fig. 5*B*).

We first asked whether acute ex vivo wash-in of the anti-TWEAK mAb would reverse the synaptic deficits in HC slices from WT DH-MCAO mice (Fig. 5 *A* and *C*). We found that anti-TWEAK mAb wash-in significantly increased the amplitudes of fEPSPs in both sham (~29%) and DH-MCAO (~29%) animals compared to their control protein-treated groups (Fig. 5 *D* and *E*). Notably, the LTP deficit in WT stroke animals was reversed by anti-TWEAK mAb wash-in compared to control protein-treated mice at 12 wk post stroke (Fig. 5 *F* and *G*).

Having established that acute pharmacological inhibition of TWEAK/Fn14 signaling can improve deficits in synaptic transmission
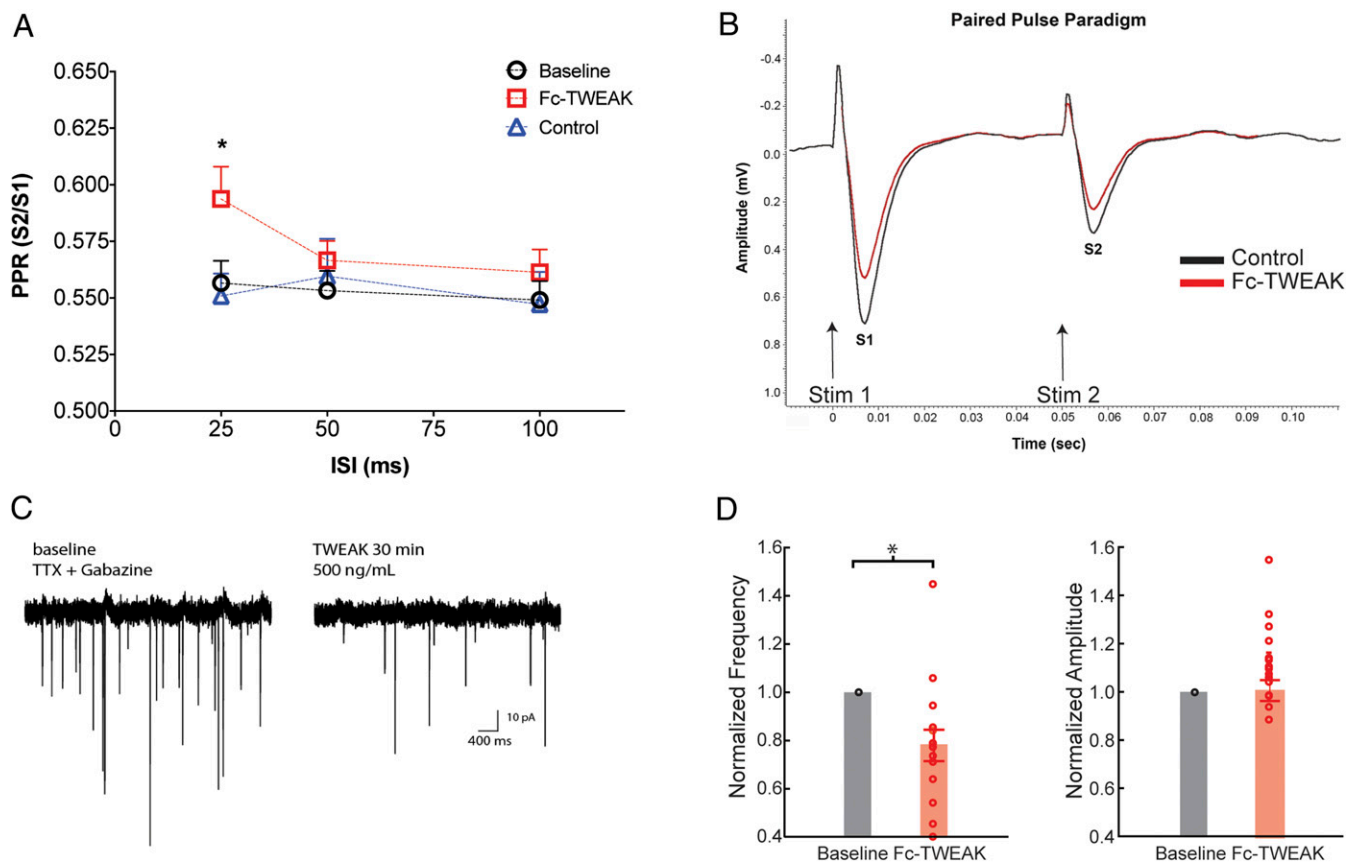
Nagy et al.
Developmental synaptic regulator, TWEAK/Fn14 signaling, is a determinant of synaptic function in models of stroke and neurodegeneration

PNAS | 5 of 11
https://doi.org/10.1073/pnas.2001679118

Fig. 3. TWEAK attenuates synaptic transmission through presynaptic mechanisms. (*A*) Paired-pulse recordings showing the ratio of the second to the first fEPSP (S2/S1) using 25-, 50-, and 100-ms ISIs at baseline and after control protein (1 µg/mL) or Fc-TWEAK (0.5 µg/mL) ex vivo wash-in in HC slices from 6- to 8-wk-old male and female WT mice. n = 6 to 10 slices/group. Data are expressed as the mean ± SEM. One-way ANOVA, Tukey's multiple comparisons test. *$P \leq 0.05$, compared to control protein-treated group. (*B*) Representative traces of paired-pulse recordings showing the first (S1) and the second (S2) fEPSPs with 50-ms ISI after control protein or Fc-TWEAK wash-in. (*C*) Representative mEPSC recording traces in baseline conditions and following TWEAK wash-in. (*D*) Quantification of mEPSC recordings. Data points from individual neurons, frequencies, and amplitudes normalized to baseline. Paired t test. *$P \leq 0.05$.

and plasticity, we next investigated if global Fn14 reduction would protect against DH-MCAO–induced neurophysiological deficits. Fn14 deletion did not affect infarct size at 24 h poststroke, suggesting that Fn14 did not mediate acute protection from cell death in this model (Fig. 5 *I* and *J*). This finding contrasts with the reduced infarct volume observed in Fn14KO mice in a different stroke model, D-MCAO (27), possibly reflecting the increased severity of our model due to postocclusion hypoxia (i.e., DH-MCAO vs. D-MCAO). However, when we examined synaptic function in hippocampal slices from DH-MCAO mice at 8 to 12 wk post stroke, we found that Fn14KO mice had a significant improvement (~28%) in basal synaptic transmission following DH-MCAO compared to WT animals, albeit not to the levels of the sham-operated control group (Fig. 5 *K* and *L*). Remarkably, Fn14 deletion completely protected against the stroke-induced LTP deficit observed in the HC slices from WT littermates at 12 wk post stroke (Fig. 5 *M* and *N*).

In order to avoid potential effects of Fn14 deficiency throughout embryonic development, we again employed nFn14KD and nScr mice (P0 injections of PHP.eB-hSYN1-GFP-shTnfrsf12a or PHP.eB-hSYN1-GFP-shScrambled). Male mice were subjected to DH-MCAO stroke at 16 wk of age, followed by ex vivo slice recordings 8 to 10 wk later (*SI Appendix*, Fig. S9A). At this time point (24 to 25 wk post shRNA injection), we observed a 42% reduction of Fn14 messenger RNA in nFn14KD compared to nScr mice (*SI Appendix*, Fig. S9B), which is similar to the knockdown observed at 6 to 8 wk post injection (*SI Appendix*, Fig. S4B). Importantly,

nFn14KD significantly improved the DH-MCAO–induced deficits in both basal synaptic transmission and LTP (*SI Appendix*, Fig. S9 *E* and *F*), confirming that postnatal neuronal Fn14 reduction is sufficient to impact the pathophysiology in the DH-MCAO stroke model.

Notably, our results using three independent approaches indicate that inhibition of TWEAK/Fn14 signaling with blocking antibodies or via genetic down-regulation of Fn14 protects from deficits in synaptic transmission and plasticity that manifest after ischemic stroke.

Discussion

Here, we provide evidence that TWEAK signaling acutely and dose-dependently reduces basal synaptic transmission and plasticity via neuronally expressed Fn14 in the mature CNS. Neurophysiologically, we link TWEAK/Fn14 signaling to presynaptic mechanisms, while phosphoproteomic analyses suggest a global modulatory role of synaptic machinery. In two independent disease models, characterized in part by synaptic dysfunction (Aβ overexpression and ischemic stroke), we find that pharmacological TWEAK blockade enhances synaptic transmission, highlighting a role for endogenous TWEAK. Finally, we demonstrate that genetic ablation of Fn14 normalizes chronic ischemic stroke-induced neurophysiological deficits. Our results support targeting the TWEAK/Fn14 pathway as a potential therapeutic approach to augment synaptic function.
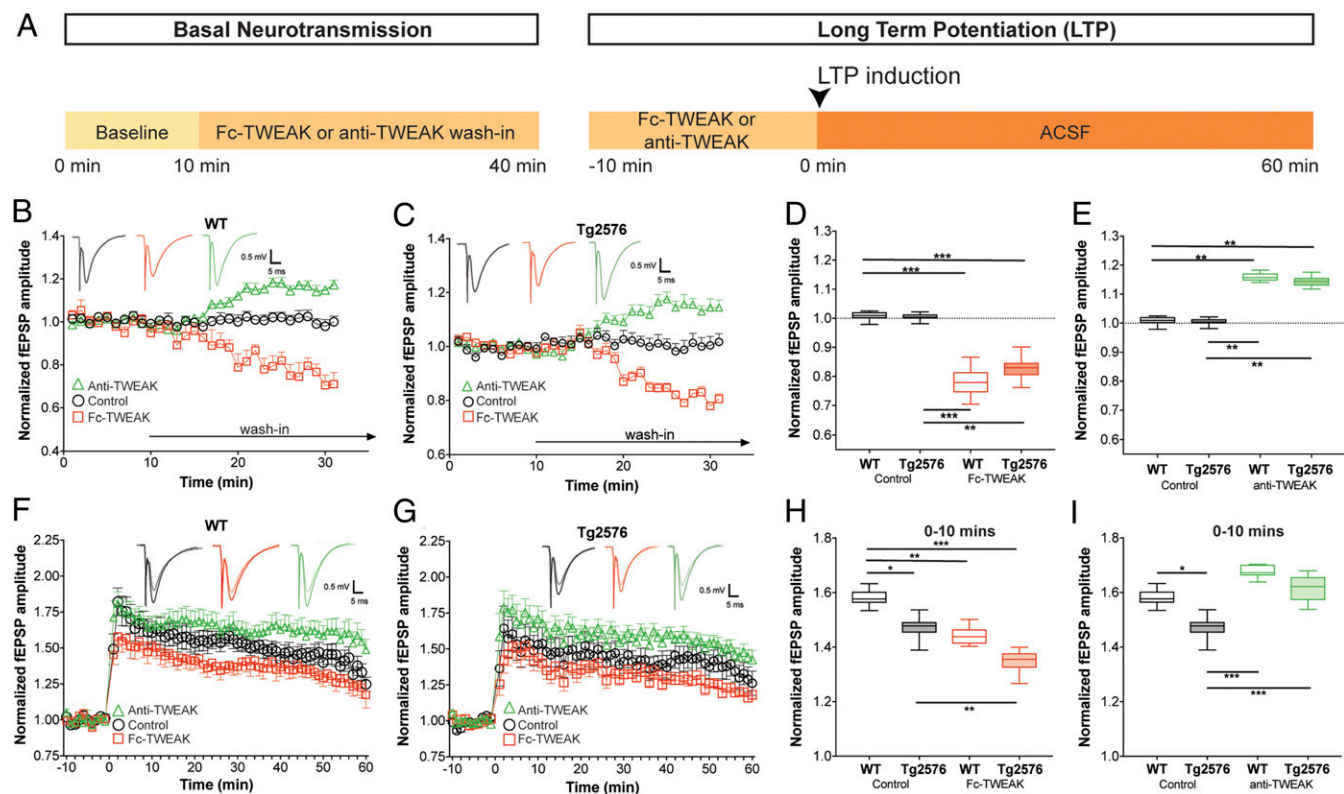
Fig. 4. Blocking TWEAK augments basal synaptic transmission and plasticity in WT and Tg2576 animals. (*A*) Schematic time line of compound wash-in and electrophysiological recordings. (*B–I*) HC slices were prepared from 9-mo-old male and female mice and treated with control protein (1 µg/mL), Fc-TWEAK (0.5 µg/mL), or anti-TWEAK (3 µg/mL). *n* = 8 to 10 slices/group. (*B* and *C*) Relative changes in basal neurotransmission in WT (*B*) and Tg2576 (*C*) mice. Group means plotted ± SEM. Representative fEPSP traces are shown. (*D* and *E*) Quantification of the changes in basal neurotransmission in WT or Tg2576 mice. Box plots show the minimum to maximum values and means of the last 10 min of the wash-in period. Dotted lines indicate the prewash-in baseline levels. Two-way ANOVA, Tukey's multiple comparisons test. **$P \le 0.01$, ***$P \le 0.001$. (*F–G*) Time line of LTP recordings in WT (*F*) and Tg2576 (*G*) mice. Group means plotted ± SEM. Representative fEPSP traces are shown. Semitransparent traces represent signals from baseline while solid traces show post-TBS signals. (*H–I*) Quantification of the LTP recordings in WT or Tg2576 mice. Box plots show the minimum to maximum values and means of the initial period (0 to 10 min) after LTP induction. Two-way ANOVA, Tukey's multiple comparisons test. *$P \le 0.05$, **$P \le 0.01$, ***$P \le 0.001$.

Our experiments delineated the ability of TWEAK to acutely regulate synaptic transmission and plasticity. We found that Fc-TWEAK wash-in acutely decreases the amplitudes of fEPSPs and the inducibility of LTP in WT, but not in Fn14KO or nFn14KD hippocampus, suggesting that TWEAK-induced modulation of synaptic functions is mediated by its interaction with neuronal Fn14. Our phosphoproteomics analysis revealed TWEAK-induced changes in phosphoproteome, with nearly half of these changes also altered by CNQX (*SI Appendix*, Table S1), an AMPA receptor antagonist used as a positive control to reduce glutamatergic synaptic transmission. MetaCore enrichment further verified that the TWEAK/Fn14-altered underlying molecular processes are highly synaptic enriched (*SI Appendix*, Table S2C), pointing to the association with synaptic transmission. In another report, it was shown that intracerebroventricular administration of TWEAK in adult mice can acutely trigger neuronal apoptosis leading to depression-like behavior and cognitive dysfunction (28). However, the ability of TWEAK to induce cell death is generally relatively weak and requires long exposure time (9) or combination with other agents such as gamma-interferon (8, 29). Indeed, in our study, we found that the decrease in synaptic function by a short 30-min TWEAK wash-in was reversible, indicating that the acute dampening in basal synaptic neurotransmission and plasticity is not the consequence of cell death. Our additional control experiment revealed that synaptic plasticity was significantly lower in the TWEAK-treated group compared to the control protein-treated

group even after the fEPSPs were readjusted to the prewash-in (baseline) levels before LTP induction. Furthermore, the lowest dose of TWEAK tested failed to impact the amplitude of fEPSPs while it significantly decreased LTP inducibility, suggesting that the effects of TWEAK on basal neurotransmission and synaptic plasticity are separable.

Importantly, we demonstrate that anti-TWEAK wash-in to WT HC slices acutely improves basal neurotransmission and synaptic plasticity, supporting the regulatory role of endogenous TWEAK in synapse physiology in the healthy brain. Moreover, both anti-TWEAK treatment of WT DH-MCAO brain slices and Fn14 deficiency (genetic or via shRNA knockdown) in mice reverses the synaptic deficits observed in the DH-MCAO model of stroke, confirming a role for endogenous TWEAK/Fn14 in this disease context. Although naive Fn14KO and nFn14KD mice showed basal neurotransmission and synaptic plasticity responses comparable to WT mice, suggesting that developmental Fn14 deficiency results in compensation, they had a significant effect in the challenging circumstance of DH-MCAO. Therefore, both the present study and that of Cheadle et al. (17) identify circumstances with significant TWEAK/Fn14 impact on synaptic function following ischemic stroke and during the visual critical period, respectively. Taken together, these disparate model systems suggest that the TWEAK/Fn14 system is tuned to periods of substantial change in neuronal activity levels (eye opening) or environment (ischemic stroke).
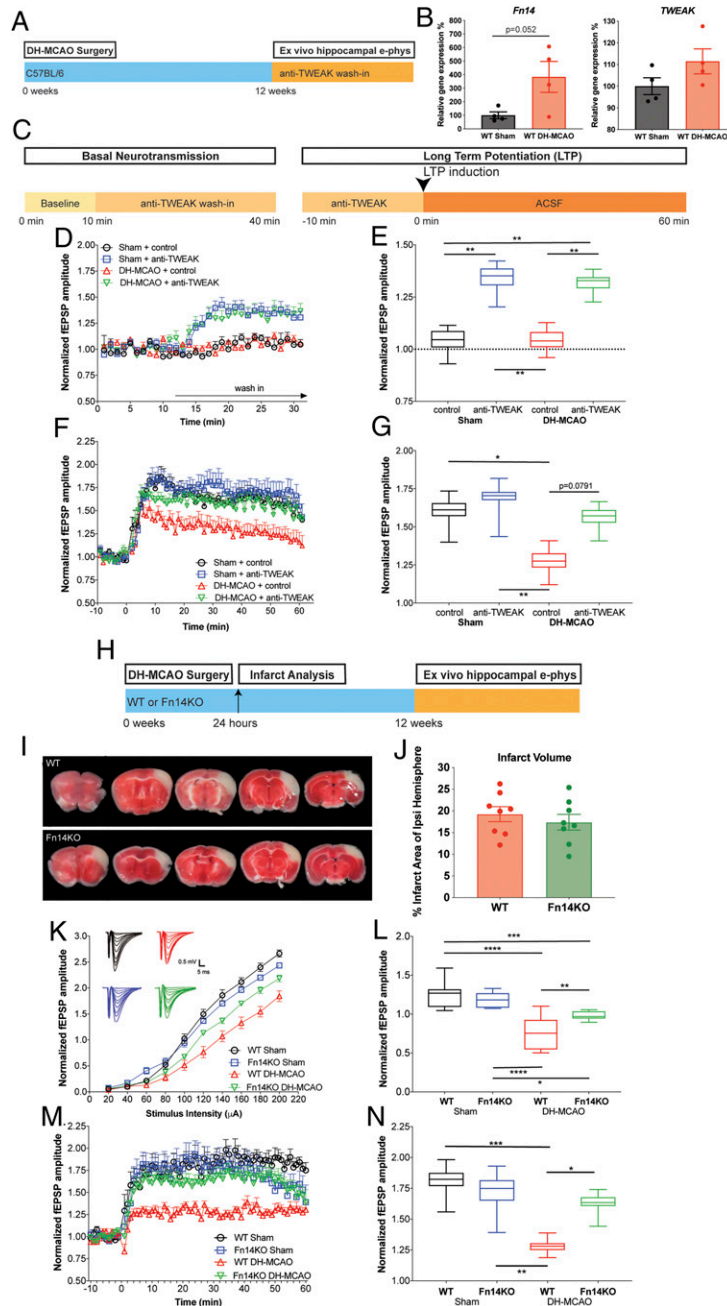
Nagy et al.
Developmental synaptic regulator, TWEAK/Fn14 signaling, is a determinant of synaptic function in models of stroke and neurodegeneration

PNAS | 7 of 11
https://doi.org/10.1073/pnas.2001679118

NEUROSCIENCE

Fig. 5. Inhibition of TWEAK/Fn14 protects against synaptic transmission deficits following ischemic stroke. (A) Schematic of DH-MCAO studies. Mice were subjected to DH-MCAO or Sham surgery at 16–18 wk of age, then aged 12 wk post surgery prior to preparation of HC slices. (B) Quantification of TWEAK and Fn14 gene expression levels by qPCR shows up-regulation of Fn14 and TWEAK in acute HC slices prepared 12 wk after DH-MCAO. $n = 4$ animals per condition. Group means plotted with individual data points, ± SEM. Unpaired t test. (C) Schematic time line of compound wash-in and electrophysiological recordings. (D and E) HC slices were prepared from male C57BL/6 WT mice 12 wk post DH-MCAO/Sham, followed by ex vivo wash-in of control protein (1 μg/mL) or anti-TWEAK (3 μg/mL). Recordings were performed from the HC ipsilateral to the stroke. $n = 6$ slices/group. (D) Relative changes in basal neurotransmission. Group means plotted ± SEM. (E) Quantification of changes in basal neurotransmission. Box plots show the minimum to maximum values and means of the last 10 min of the wash-in period. Dotted line indicates the prewash-in baseline levels. Two-way ANOVA, Tukey's multiple comparisons test. **$P \le 0.05$. (F) Time line of LTP recordings. Group means plotted ± SEM. (G) Quantification of LTP recording. Box plots show the minimum to maximum values and means of the 10- to 50-min period after LTP induction. Two-way ANOVA, Tukey's multiple comparisons test. *$P \le 0.05$, **$P \le 0.01$. (H) Schematic of DH-MCAO surgery in male WT or Fn14KO animals at 16 to 18 wk of age. Infarct analysis was preformed 24 h after surgery, and animals were aged 12 wk post surgery prior to analysis. (I) Representative 1-mm coronal slices of WT and Fn14KO animals 24 h post DH-MCAO stained with TTC to visualize infarct region. (J) Quantification of infarcted region as measured by percentage of metabolically inactive area within the ipsilateral hemisphere. $n = 8$ mice/genotype. Group means plotted with individual animal data ± SEM. Unpaired t test. There is no significant difference between WT and Fn14KO. (K–N) HC slices were prepared from male WT or Fn14KO mice 12 wk post DH-MCAO/Sham. $n = 6$ to 8 slices/group. (K) Basal neurotransmission evaluated by input/output curves at hippocampal CA1 ipsilateral to the stroke. Group means plotted ± SEM. (L) Quantification of input/output curves. Box plots show the minimum to maximum values and means of the higher stimulus intensities (100 to 200 μA) ± SEM. Two-way ANOVA, Tukey's multiple comparisons test. *$P \le 0.05$, **$P \le 0.01$, ***$P \le 0.001$, ****$P \le 0.0001$. (M) Time line of LTP recordings performed ipsilateral to the stroke. Group means plotted ± SEM. (N) Quantification of LTP recordings. Box plots show the minimum to maximum values and means of the 10- to 50-min period after LTP induction ± SEM. Repeated measures two-way ANOVA, Tukey's multiple comparisons test. *$P \le 0.05$, **$P \le 0.01$, *** $P \le 0.001$.

Nagy et al.
Developmental synaptic regulator, TWEAK/Fn14 signaling, is a determinant of synaptic
function in models of stroke and neurodegeneration

To investigate mechanistically the TWEAK/Fn14 effects on synaptic transmission, we employed two independent electrophysiological approaches and a proteomic analysis. We found that TWEAK wash-in increased the PPR in ex vivo HC slices and specifically reduced the frequency of spontaneous mEPSCs. Both results indicate decrease in neurotransmitter release probability and suggest that acute TWEAK exposure can modulate synaptic physiology through presynaptic mechanisms, which could include decreased calcium influx, inactivation of release sites, and vesicle depletion (30). Unbiased phosphoproteomic analysis supports this view, identifying a set of differentially phosphorylated presynaptic proteins such as SYN1/3 and CACNAB1, which could account for deficits in presynaptic function in both action potential-dependent (PPR) and -independent (mEPSC) assays. Importantly, phosphoproteomic analysis revealed that TWEAK treatment also changes the phosphorylation states of a large set of postsynaptic proteins such as SHANK1/3- and PSD-95-associated proteins. Interestingly, the functional network-building analysis (*SI Appendix*, Fig. S2C) showed that TWEAK/Fn14 affects synaptic function possibly via Rac1 and/or Traf2, consistent with the role of Rac1 in LTP (31) and a prior report of Rac1-dependent Fn14 regulation of actin cytoskeletal reorganization directly or indirectly via a TRAF adaptor protein (32).

Having established an acute role for TWEAK/Fn14 regulation of broad synaptic function in adult mice, we investigated whether the TWEAK/Fn14 pathway modulates synaptic function in models of neurological disorders. For our current study, we chose two different disease contexts, namely models of AD and ischemic stroke, given that AD and ischemic stroke patients exhibit significant up-regulation of TWEAK and/or Fn14 expression in their CNS or cerebrospinal fluid (14–16).

Tg2576 mice are a well-described model of AD that exhibit synaptic pathophysiology due to Aβ overexpression (24, 25). Although this animal model is widely used to study amyloid-dependent synaptic dysfunctions, reported findings vary regarding the extent to which basal neurotransmission and LTP are affected (33–37). Possible explanations for the high variability in this model include differences in the age of the Tg2576 animals and various experimental parameters (38). Our functional characterization of aged 9-mo-old Tg2576 mice revealed reduced basal neurotransmission and synaptic plasticity compared to age-matched WT mice; however, the decrease in LTP reached significant levels only at the early initial phase (0 to 10 min), which can be considered a short-term plasticity effect. While ex vivo wash-in of Fc-TWEAK further deteriorated these synaptic functions, our data indicate that inhibition of the pathway by acute anti-TWEAK wash-in improves basal neurotransmission and synaptic plasticity in both WT and Tg2576 mice, normalizing the LTP induction phase in the latter. Our findings suggest that TWEAK/Fn14 signaling retains a synaptic modulatory capacity in aging and AD-like synaptic pathophysiology without an Aβ-dependent exaggeration of the TWEAK/Fn14 synaptic effect. Given that synapse loss is correlated with cognitive dysfunction in AD patients (39), we speculate that tempering this pathway may be beneficial for improving cognitive deficits associated with AD either by acutely augmenting synaptic transmission and/or reducing further synaptic deficits.

Strikingly, we found that TWEAK/Fn14 signaling is necessary for the deficits in synaptic transmission and plasticity that manifest after ischemic stroke. To delineate this pathophysiological contribution of the TWEAK/Fn14 axis, we leveraged a model featuring delayed impairment of neuronal activity that could be detected in HC slices after ischemic infarction of the somatosensory cortex in DH-MCAO mice. Infarct volume, which is due to excitotoxic cell death, was unaltered by genetic loss of TWEAK/Fn14 signaling in this model. The initial infarction is followed by dynamic regional changes in the surviving neurons over the course of weeks, including changes in basal neurotransmission and plasticity in the hippocampus (40). Therefore, we investigated whether a loss of TWEAK/Fn14 signaling would protect against ischemic stroke-induced synaptic pathophysiology. In agreement with previous studies, we found a significant unilateral attenuation of hippocampal basal neurotransmission and plasticity 12 wk post stroke. Multiple lines of evidence suggest that inhibition of TWEAK/Fn14 signaling can rescue poststroke synaptic deficits. Acute pharmacological inhibition of TWEAK signaling post stroke increased basal synaptic transmission and plasticity. Additionally, genetic ablation of TWEAK/Fn14 signaling in the Fn14KO mice and down-regulation of Fn14 with shRNA in nFn14KD mice rescued deficits in basal synaptic transmission and returned LTP magnitude to close to normal levels. Interestingly, Fn14 knockdown by ∼40% was sufficient for this beneficial effect on stroke-induced electrophysiological deficits. Together, these data suggest aberrant activation of TWEAK/Fn14 signaling is necessary for synaptic dysfunction in ischemic stroke and that inhibition of this pathway in the context of synaptic dysfunction is restorative.

Other prominent cytokines, such as interleukin-1 beta (IL-1β) and tumor necrosis factor alpha (TNFα), appear up-regulated in microglia and/or macrophages after ischemic stroke (41) where they contribute to neuronal death (42). These cytokines have also been reported to modulate synaptic function, supporting a paradigm in which glial cells secrete immune-related signaling molecules that alter synaptic transmission and plasticity (43, 44). The enrichment of TWEAK in microglia reported by others (18, 19) and our finding that TWEAK regulates synaptic function through neuronal Fn14 suggest that a glial–neuronal axis fits this paradigm. Importantly, TWEAK/Fn14 signaling is a nonredundant determinant of synaptic function after ischemic stroke and in AD models.

In summary, we identified TWEAK/Fn14 signaling as a distinct modulator of synaptic physiology and pathophysiology in the mature brain. We propose that this pathway, which is normally activated during visual development, remains active in contexts of aging and neurodegenerative diseases and is engaged under challenging circumstances, such as in ischemic stroke, and contributes to synaptic dysfunction in these disorders. Therefore, our data suggest that inhibition of TWEAK/Fn14 signaling could have broad therapeutic potential to normalize neuropathophysiological changes observed in aging, Alzheimer's disease, ischemic stroke, and potentially other disorders featuring synaptic deficits.

Materials and Methods

Experimental Models and Subject Details. All animal experiments were performed in compliance with protocols approved by the Institutional Animal Care and Use Committee at Biogen (protocols #780, #660, and #820). All animals were housed under standard conditions in ventilated cages on a 12-h light/dark cycle and provided food and water ad libitum. Dose–response experiments used male and female C57BL/6 mice supplied by Jackson Laboratories (catalog #000664). No apparent sex differences were detected between male and female mice in response to Fc-TWEAK wash-in. Male B6;SJL-Tg(APPSWE)2576Kha (TG2576) (45) hemizygous mice with appropriate WT littermate controls were supplied by Taconic Farms (catalog #1349). Male mice deficient in the TWEAK receptor Fn14, known as B6.Tnfrsf12a$^{tm1(KO)Biogen}$ (Fn14KO) (20), were bred from a heterozygous cross; KO and WT littermate controls were used for experiments. For some experiments, P0 pups from C57BL/6 timed matings were injected with viral vectors with nFn14KD or control scrambled vector (nScr). The ages of the mice used for each experiment are specified in the figure legends.

Recombinant Proteins and Antibodies. Recombinant murine Fc-TWEAK fusion protein and anti-mouse TWEAK monoclonal antibody (clone mP2D10) were generated by Biogen as described (46). An irrelevant isotype-matched control protein, anti-hen egg lysozyme, mIgG2a subclass, was generated by Biogen using standard methods. Aglycosylated murine Fc-TWEAK fusion protein, agly-Fc-TWEAK, was similarly constructed but with the N297Q muIgG1 Fc sequence, thereby creating an Fc-effector function-deficient protein.

Brain Slice Electrophysiology.

Acute slice preparation. Animals were decapitated with a guillotine and brains were rapidly dissected in ice-cold media consisting of 228 mM sucrose, 26 mM NaHCO₃, 10 mM glucose, 7.0 mM MgSO₄, 2.5 mM KCl, 1.0 mM NaH₂PO₄, and

Nagy et al.
Developmental synaptic regulator, TWEAK/Fn14 signaling, is a determinant of synaptic function in models of stroke and neurodegeneration

PNAS | 9 of 11
https://doi.org/10.1073/pnas.2001679118

NEUROSCIENCE

0.5 mM CaCl$_2$, equilibrated with 95% O$_2$ and 5% CO$_2$ (carbogen). The forebrain was mounted to a cutting stage and 350-µm-thick coronal slices containing the hippocampus were prepared using a vibratome (Leica, VT 1000 S). Slices were transferred to an incubation chamber containing artificial cerebrospinal fluid (ACSF) consisting of 122 mM NaCl, 26 mM NaHCO$_3$, 11 mM glucose, 2.5 mM CaCl$_2$, 2.5 mM KCl, 1.3 mM MgCl$_2$, and 1.0 mM NaH$_2$PO$_4$ and constantly saturated with carbogen. Slices were incubated for at least 60 to 90 min at room temperature (22 °C) before use. Experiments were performed 1 to 6 h after the incubation period. Slices were transferred to a temperature-controlled submerged type recording chamber continuously perfused (2 to 3 mL/min) with heated (32°C to 33 °C) and carbogen-saturated ACSF containing 10 mM glucose, 126 mM NaCl, 2.5 mM KCl, 1.25 mM NaH$_2$PO$_4$, 1.3 mM MgCl$_2$, 2.5 mM CaCl$_2$, and 26 mM NaHCO$_3$, pH 7.4. The fEPSPs were recorded from the stratum radiatum of the hippocampal CA1 subregion using a glass recording electrode filled with ACSF with resistances ranging from 1 to 3 MΩ. A concentric bipolar tungsten stimulating electrode (WPI) was placed in the CA1 Shaffer-collaterals ~200 µm retrograde from the recording electrode. A detailed description of data acquisition and analysis are included in *SI Appendix, Materials and Methods*.

Synaptic Current Recordings from Primary Mouse Neurons. The mEPSCs were recorded in dissociated mouse cortical cultures. Embryonic day 18 (E18) mouse cortex was dissociated, and 125,000 neurons were plated on 25-mm poly-D-lysine–coated coverslips. Cultures were maintained in BrainPhys media (Stem Cell Technologies) for 18 to 21 d before recordings. Coverslips were transferred to a recording chamber perfused with room temperature, carbogen-saturated (95%O$_2$/5%CO$_2$) recording ACSF (~1 mL/min) containing 1 µM tetrodotoxin and 10 µM Gabazine for 10 min prior to recordings. Whole-cell recordings were performed with thick-walled borosilicate glass pipettes pulled to a resistance of 3 to 5 MΩ and filed with 130 mM cesium methanesulfonate, 10 mM CsCl, 10 mM Hepes, 4 mM Mg-ATP, 0.3 mM Na-GTP, 0.2 mM EGTA, 10 mM Na-phosphocreatine, adjusted to pH 7.2. Further details of data acquisition and analysis are provided in *SI Appendix, Materials and Methods*.

Phosphoproteomics. Brain-slice samples from 6- to 8-wk-old male WT and Fn14KO mice were treated with Fc-TWEAK or CNQX, an AMPA receptor antagonist used as a positive control for reduction of glutamatergic synaptic transmission, for 30 min according to the same experimental design and conditions as in the electrophysiology study (Fig. 1A). Six biological replicates per treatment condition in WT or Fn14KO mice were subjected to TMT (47) labeling-coupled phosphoproteomics study. Further details about sample processing and data analysis are provided in *SI Appendix, Materials and Methods*.

Neuronal Knockdown of Tnfrsf12a (Fn14) Using Viral Vectors in Mice. Neuronal specific knockdown of *Tnfrsf12a* (gene alias name, Fn14) was achieved through use of viral vectors expressing shRNA targeting *Tnfrsf12a*: PHP.eB-hSYN-GFP-shTnfrsf12a. Two hairpins used to knock down expression of murine *Tnfrsf12a* (NM_013749) were cloned into a Pol II expression system downstream of the human synapsin-1 promoter-driven GFP reporter gene to restrict the knockdown to neurons. The shRNA sequences are the following: 5′-GCTGACCAGGAAACTAGAAACCAGCGTTTTGGCCACTGACGCTGGTT-TGTTTCCTGGTCAG-3′ and 5′-GCTGGAATGAATGAATGGACGACGA.GTTTTG-GCCACTGACTGACTCGTCGTCTTCATTCATTCCAG-3′. These target NM_013749 bases 303 to 323 in the open reading frame and 438 to 458 in the 3′ untranslated region, respectively. The cloning and packaging were performed by Vector Biolabs. Viral expression constructs were generated by packaging a 1:1 mix of the two vector plasmids in AAV9 with the PHP.eB capsid modification (48), resulting in the PHP.eB-hSYN1-GFP-shTnfrsf12a viral vector. A similarly constructed viral vector with a scrambled sequence (PHP.eB-hSYN1-GFP-shScrambled) served as a control. These viral vectors were injected into the ventricles of P0 C57BL/6 mice to generate mice with neuronal knockdown of *Tnfrsf12a* (nFn14KD) or controls (nScr). P0 pups were anesthetized on ice until unresponsive by toe pinch. For intracerebroventricular injections, pups were injected at a 30° angle from the head, halfway

between lambda and bregma, 1 mm lateral from the midline suture, with 2 mm depth. Injections were performed bilaterally with 2 µL/injection using a Hamilton gas-tight syringe (1701 RN) with custom 33-gauge, 45 degree-beveled needles (9.5 mm, catalog #7803–05). The viral vectors were injected at 7.5 E12 gc/mL in a solution of 10% Fast-Green dye (Electron Microscopy Sciences, catalog #26364–05). An injection was considered successful if vector dye was visualized in both ventricles. Immediately following injections, pups were warmed on a closed-circulation heating pad until fully recovered, rolled around in cage bedding, and returned to the original cage with the mother. A detailed description of evaluation of Fn14 expression in mice injected with the PHP.eB-hSYN1-GFP-shTnfrsf12a viral vector is included in *SI Appendix, Materials and Methods*.

DH-MCAO Surgery and Quantification of Infarct. Male 14- to 16-wk-old C57BL/6 WT and Fn14KO littermates and male 16- to 18-wk-old nScr and nFn14KD mice were used for distal middle cerebral artery occlusion (DMCAO) as previously described (49), followed by 1 h of hypoxia (8% oxygen and 92% nitrogen), with the hypoxia chamber maintained at 37 °C to prevent hypothermia. This combination of DMCAO + hypoxia (DH-MCAO) produces a more reproducible and larger infarct size as compared to DMCAO (49). Sham surgeries were identical to stroke surgeries except for the lack of cauterization of the middle cerebral artery. Infarcted regions were visualized 24 h after DH-MCAO surgery using 2,3,5-triphenyltetrazolium chloride (TTC) (Sigma-Aldrich, catalog #17779) as previously described (40). Brains were extracted and sliced coronally into 1-mm sections, for a total of eight to nine sections spanning the length of the infarcted regions. Free-floating slices were then stained for 15 min at room temperature in 1 mL of 1.5% TTC solution in phosphate-buffered saline and then transferred to a 10% formalin solution to stop the reaction. Slices were then imaged and analyzed using NIH ImageJ to quantify the area of infarct cortex in the ipsilateral hemisphere. Infarct quantification is expressed as percentage of the infarcted region of the total ipsilateral hemisphere. For volumetric quantifications, measurements were multiplied by the distance between sections (1 mm) and summed across the entire brain for infarct measurement. The experimenter was blinded to the genotypes.

Quantification and Statistical Analysis. For electrophysiological experiments, the details of data acquisition are described in *SI Appendix, Materials and Methods*. Analysis of fEPSPs and EPSCs was done in Spike 2 version 8 (Cambridge Electronic Design), Clampfit (Molecular Devices), and Prism 7 (GraphPad Software). For histological experiments, analysis of IBA-1 and GFAP was performed with custom image analysis algorithms using Visiopharm image analysis software; additional data acquisition details are described in *SI Appendix, Materials and Methods*. Density of dendritic spines was calculated in Excel by dividing spine number over dendrite length. Statistical analysis for spine density was performed using Matlab (Math-Works). All electrophysiology, histology, dendritic spine density, and stroke experiments were performed blinded to genotype and treatment condition. All treatments and the order of the recordings were randomized. All statistical analyses for electrophysiology experiments were performed using Prism 7 software. The statistical analyses and "*n*" numbers for each experiment are given in the figure legends. Data analysis was performed blinded to genotypes. Error bars represent SEM. Statistical significance in plots is indicated with *$P \leq 0.05$, **$P \leq 0.01$, ***$P \leq 0.001$, and ****$P \leq 0.0001$.

1. P. D. Coleman, P. J. Yao, Synaptic slaughter in Alzheimer's disease. *Neurobiol. Aging* **24**, 1023–1027 (2003).
2. I. Feinberg, Schizophrenia: Caused by a fault in programmed synaptic elimination during adolescence? *J. Psychiatr. Res.* **17**, 319–334 (1982-1983).
3. M. S. Thomas, R. Davis, A. Karmiloff-Smith, V. C. Knowland, T. Charman, The over-pruning hypothesis of autism. *Dev. Sci.* **19**, 284–305 (2016).
4. S. Hong *et al.*, Complement and microglia mediate early synapse loss in Alzheimer mouse models. *Science* **352**, 712–716 (2016).
5. P. Cicinelli, R. Traversa, P. M. Rossini, Post-stroke reorganization of brain motor output to the hand: A 2-4 month follow-up with focal magnetic

transcranial stimulation. *Electroencephalogr. Clin. Neurophysiol.* **105**, 438–450 (1997).
6. T. H. Murphy, D. Corbett, Plasticity during stroke recovery: From synapse to behaviour. *Nat. Rev. Neurosci.* **10**, 861–872 (2009).
7. B. H. Dobkin, Clinical practice. Rehabilitation after stroke. *N. Engl. J. Med.* **352**, 1677–1684 (2005).
8. Y. Chicheportiche *et al.*, TWEAK, a new secreted ligand in the tumor necrosis factor family that weakly induces apoptosis. *J. Biol. Chem.* **272**, 32401–32410 (1997).
9. J. A. Winkles, The TWEAK-Fn14 cytokine-receptor axis: Discovery, biology and therapeutic targeting. *Nat. Rev. Drug Discov.* **7**, 411–425 (2008).

10 of 11 | PNAS
https://doi.org/10.1073/pnas.2001679118

Nagy et al.
Developmental synaptic regulator, TWEAK/Fn14 signaling, is a determinant of synaptic function in models of stroke and neurodegeneration

10. L. C. Burkly, J. S. Michaelson, T. S. Zheng, TWEAK/Fn14 pathway: An immunological switch for shaping tissue responses. *Immunol. Rev.* **244**, 99–114 (2011).
11. M. Allen *et al.*, Human whole genome genotype and transcriptome data for Alzheimer's and other neurodegenerative diseases. *Sci. Data* **3**, 160089 (2016).
12. P. L. De Jager *et al.*, A multi-omic atlas of the human frontal cortex for aging and Alzheimer's disease research. *Sci. Data* **5**, 180142 (2018).
13. M. Wang *et al.*, The Mount Sinai cohort of large-scale genomic, transcriptomic and proteomic data in Alzheimer's disease. *Sci. Data* **5**, 180185 (2018).
14. I. Inta *et al.*, Induction of the cytokine TWEAK and its receptor Fn14 in ischemic stroke. *J. Neurol. Sci.* **275**, 117–120 (2008).
15. I. Potrovita *et al.*, Tumor necrosis factor-like weak inducer of apoptosis-induced neurodegeneration. *J. Neurosci.* **24**, 8237–8244 (2004).
16. M. Yepes *et al.*, A soluble Fn14-Fc decoy receptor reduces infarct volume in a murine model of cerebral ischemia. *Am. J. Pathol.* **166**, 511–520 (2005).
17. L. Cheadle *et al.*, Visual experience-dependent expression of Fn14 is required for retinogeniculate refinement. *Neuron* **99**, 525–539.e10 (2018).
18. L. Cheadle *et al.*, Sensory experience engages microglia to shape neural connectivity through a non-phagocytic mechanism. *Neuron* **108**, 451–468.e9 (2020).
19. Y. Zhang *et al.*, An RNA-sequencing transcriptome and splicing database of glia, neurons, and vascular cells of the cerebral cortex. *J. Neurosci.* **34**, 11929–11947 (2014).
20. M. Girgenrath *et al.*, TWEAK, via its receptor Fn14, is a novel regulator of mesenchymal progenitor cells and skeletal muscle regeneration. *EMBO J.* **25**, 5826–5839 (2006).
21. D. Fioravante, W. G. Regehr, Short-term forms of presynaptic plasticity. *Curr. Opin. Neurobiol.* **21**, 269–274 (2011).
22. J. Del Castillo, B. Katz, Quantal components of the end-plate potential. *J. Physiol.* **124**, 560–573 (1954).
23. S. Redman, Quantal analysis of synaptic potentials in neurons of the central nervous system. *Physiol. Rev.* **70**, 165–198 (1990).
24. T. Ondrejcak *et al.*, Alzheimer's disease amyloid beta-protein and synaptic function. *Neuromolecular Med.* **12**, 13–26 (2010).
25. J. Pozueta, R. Lefort, M. L. Shelanski, Synaptic changes in Alzheimer's disease and its models. *Neuroscience* **251**, 51–65 (2013).
26. K. P. Doyle *et al.*, B-lymphocyte-mediated delayed cognitive impairment following stroke. *J. Neurosci.* **35**, 2133–2145 (2015).
27. X. Zhang *et al.*, TWEAK-Fn14 pathway inhibition protects the integrity of the neurovascular unit during cerebral ischemia. *J. Cereb. Blood Flow Metab.* **27**, 534–544 (2007).
28. J. Wen *et al.*, Intracerebroventricular administration of TNF-like weak inducer of apoptosis induces depression-like behavior and cognitive dysfunction in non-autoimmune mice. *Brain Behav. Immun.* **54**, 27–37 (2016).
29. M. Nakayama *et al.*, Multiple pathways of TWEAK-induced cell death. *J. Immunol.* **168**, 734–743 (2002).
30. R. S. Zucker, W. G. Regehr, Short-term synaptic plasticity. *Annu. Rev. Physiol.* **64**, 355–405 (2002).
31. U. Haditsch *et al.*, A central role for the small GTPase Rac1 in hippocampal plasticity and spatial learning and memory. *Mol. Cell. Neurosci.* **41**, 409–419 (2009).
32. N. L. Tran *et al.*, Increased fibroblast growth factor-inducible 14 expression levels promote glioma cell invasion via Rac1 and nuclear factor-kappaB and correlate with poor patient outcome. *Cancer Res.* **66**, 9535–9542 (2006).
33. P. F. Chapman *et al.*, Impaired synaptic plasticity and learning in aged amyloid precursor protein transgenic mice. *Nat. Neurosci.* **2**, 271–276 (1999).
34. S. M. Fitzjohn *et al.*, Age-related impairment of synaptic transmission but normal long-term potentiation in transgenic mice that overexpress the human APP695SWE mutant form of amyloid precursor protein. *J. Neurosci.* **21**, 4691–4698 (2001).
35. J. H. Jung, K. An, O. B. Kwon, H. S. Kim, J. H. Kim, Pathway-specific alteration of synaptic plasticity in Tg2576 mice. *Mol. Cells* **32**, 197–201 (2011).
36. F. Lanté *et al.*, Subchronic glucocorticoid receptor inhibition rescues early episodic memory and synaptic plasticity deficits in a mouse model of Alzheimer's disease. *Neuropsychopharmacology* **40**, 1772–1781 (2015).
37. L. Lee *et al.*, Regulation of synaptic plasticity and cognition by SUMO in normal physiology and Alzheimer's disease. *Sci. Rep.* **4**, 7190 (2014).
38. D. Fernández-Fernández, C. Dorner-Ciossek, K. S. Kroker, H. Rosenbrock, Age-related synaptic dysfunction in Tg2576 mice starts as a failure in early long-term potentiation which develops into a full abolishment of late long-term potentiation. *J. Neurosci. Res.* **94**, 266–281 (2016).
39. R. D. Terry *et al.*, Physical basis of cognitive alterations in Alzheimer's disease: Synapse loss is the major correlate of cognitive impairment. *Ann. Neurol.* **30**, 572–580 (1991).
40. K. P. Doyle, M. S. Buckwalter, A mouse model of permanent focal ischemia: Distal middle cerebral artery occlusion. *Methods Mol. Biol.* **1135**, 103–110 (2014).
41. K. L. Lambertsen, K. Biber, B. Finsen, Inflammatory cytokines in experimental and human stroke. *J. Cereb. Blood Flow Metab.* **32**, 1677–1698 (2012).
42. O. A. Sobowale *et al.*, Interleukin-1 in stroke: From bench to bedside. *Stroke* **47**, 2160–2167 (2016).
43. G. Li *et al.*, Cytokines and epilepsy. *Seizure* **20**, 249–256 (2011).
44. Y. Wu, L. Dissing-Olesen, B. A. MacVicar, B. Stevens, Microglia: Dynamic mediators of synapse development and plasticity. *Trends Immunol.* **36**, 605–613 (2015).
45. K. Hsiao *et al.*, Correlative memory deficits, Abeta elevation, and amyloid plaques in transgenic mice. *Science* **274**, 99–102 (1996).
46. S. Campbell *et al.*, Proinflammatory effects of TWEAK/Fn14 interactions in glomerular mesangial cells. *J. Immunol.* **176**, 1889–1898 (2006).
47. A. Thompson *et al.*, Tandem mass tags: A novel quantification strategy for comparative analysis of complex protein mixtures by MS/MS. *Anal. Chem.* **75**, 1895–1904 (2003).
48. K. Y. Chan *et al.*, Engineered AAVs for efficient noninvasive gene delivery to the central and peripheral nervous systems. *Nat. Neurosci.* **20**, 1172–1179 (2017).
49. K. P. Doyle, N. Fathali, M. R. Siddiqui, M. S. Buckwalter, Distal hypoxic stroke: A new mouse model of stroke with high throughput, low variability and a quantifiable functional deficit. *J. Neurosci. Methods* **207**, 31–40 (2012).
50. Y. Perez-Riverol *et al.*, The PRIDE database and related tools and resources in 2019: Improving support for quantification data. *Nucleic Acids Res.* **47**, D442–D450 (2019).

Nagy et al.
Developmental synaptic regulator, TWEAK/Fn14 signaling, is a determinant of synaptic function in models of stroke and neurodegeneration

PNAS | 11 of 11
https://doi.org/10.1073/pnas.2001679118